METEOROLOGICAL OFFICE
London Road, Bracknell, Berks.

MET.O.15 INTERNAL REPORT

No. 76

INVESTIGATION OF AN "INSTANT OCCLUSION" EVENT DURING FRONTS87

M V Young

July 1988

Cloud Physics Branch (Met.O.15)

INVESTIGATION OF AN "INSTANT OCCLUSION" EVENT DURING FRONTS87

M. V. Young

July 1988

1. INTRODUCTION

Satellite images show that over the north Atlantic, cold air vortices frequently interact and merge with polar fronts. The resulting cloud formation is often analysed as an "instant occlusion", first referred to by Anderson et al. (1969). Browning and Hill (1985) proposed a conceptual model for such events which was modified by McGinnigle et al. (MYB, 1988) to account for cases where significant baroclinicity was present in the cold air leading to cyclogenesis. In the model (Fig. 1), the "instant occlusion" is replaced by a warm front and secondary cold front associated with the cold air vortex.

This paper examines a clear case which occurred during the FRONTS87 project (Clough, 1987) when observations from an enhanced synoptic network were available. The observations have been used to confirm several important aspects of the frontal analysis and the conceptual model proposed in MYB.

The imagery for this event is compared with the somewhat similar looking "cloud-head" which frequently precedes explosive cyclogenesis (Monk and Bader, 1988). Similarities and differences in appearance are considered using numerical model cross-sections. Some aspects of the final frontal analysis are shown to resemble the split-front model of Browning and Monk (1982), and the development of deep convection is linked to the "cool wedge" idea proposed by Browning and Hill (1984).

Throughout the two days before this event guidance from the UK and ECMWF numerical models was unclear. Application of the conceptual model of MYB is shown to be important for predicting the synoptic evolution up to a day ahead.

2. SYNOPTIC SCALE EVOLUTION

The synoptic scale evolution from 4-6 January 1988 is illustrated by the sequence of NOAA satellite images in Fig. 2. Three major cloud features are identified. C and A are areas of mainly convective cloud which originated in cold, unstable air. F is a band of layered cloud accompanying a rearward-sloping cold front. The evolution of C, A, and F strongly resembled the corresponding features in the sequence of satellite images from 7-10 February 1987 indicated in Fig. 4 of MYB- namely the approach of A, and later C, to F (Fig. 2b,c), with C (and not A) eventually merging with F (Figs. 2c,d) to form one cloud system. The approach of C to F and their eventual merging conforms to the life cycle conceptual model in Fig. 1, the image in Fig. 2b occurring shortly after stage 1, and Figs. 2c and 2d corresponding to stages 2 and 3 respectively.

A and C formed within a separate baroclinic zone to the rear of F (deduced from fine-mesh model 850mb wet bulb potential temperature (WBPT) analyses), ahead of minor upper level short-wave troughs. The trough associated with C (bold dashed line in Fig. 3) moved around the amplifying mid Atlantic upper trough at 35 to 40kn, steadily approaching F. When C moved ahead of the main upper trough (Fig. 3b) it was accompanied by strong upward motion (seen on Fig. 4 west of Iberia) due to positive vorticity advection. C underwent cyclogenesis, deepening from 991mb to 976mb in the 24 hours to 00GMT 6 January as it moved northeast towards the British Isles, eventually forming an upper-level circulation (Fig. 3c). Meanwhile, A did not develop, having moved well forward of the main development area at the base of the upper trough. Moreover, warm advection dominated A (Fig. 4) implying a likely weakening of the low and its associated cloud area (Kurz, 1987).

The evolution at 500mb shown in Fig. 3 strongly resembled the cases presented in Fig. 8 of MYB. The similarity can therefore be exploited by the forecaster to identify upper-air patterns favouring the developments depicted in Fig. 1 (namely a short-wave trough embedded in a strong, amplifying upper flow pattern upwind of an historical cold front).

3. FRONTAL ANALYSIS AND MESOSCALE WEATHER DISTRIBUTION

This section concentrates on the mesoscale developments seen both in the imagery and at the surface between the times of the images shown in Figs. 2c and 2d.

Half-hourly false colour Meteosat infra-red images (Fig.5) were used to examine in more detail the following distinct changes to the cloud pattern resembling those discussed in section 2 of MYB:

(i) The upper and middle level cloud comprising the tail T of the cold air vortex (Fig 2b,c) rapidly dissipated as shown in Figs. 5a,b.

(ii)Following dissipation of T, several new curved bands of convective cloud developed between C and F (Figs. 5b-d). At the north of one such band, cloud area 1 (Fig. 5c) expanded rapidly into the eastern boundary of C, quickly followed by area 2 (Figs. 5d-f) which was an area of thunderstorms, whose upper level cloud had, by 00GMT, bridged the gap between C and F.

Although the gap between C and F appears to have been bridged much earlier west of Brest on Fig. 2c, the small middle level cloud area responsible did not persist and was not accompanied by significant rain. It is important to look for evidence of rapid convective growth to bridge the gap (giving heavy rain) rather than middle or upper level cloud which has clearly been advected from elsewhere.

The frontal analysis represents a clearly defined seqence of weather demonstrated by surface reports (Figs. 6,7) and the European radar network (Fig. 8). During 5 January, several surface pressure centres

beneath C consolidated and deepened into a single centre by 18GMT (Fig. 6a). Meanwhile, warm air was advected rapidly northwards over Biscay on its forward side. This advection had two pronounced effects. First, the thermal contrast at low-levels across the previously well-marked forward front decreased, and the front became increasingly difficult to identify at the surface (Figs. 6a,b). Secondly, warm frontogenesis occurred at the forward boundary of the warm air. This boundary is clearly marked by a wind-shift from east to south and temperature rise of 2C (Figs. 6,7) at the surface over southern England. Very strong winds- in excess of 40kn were reported over the sea near southwest England around the surface low.

The precise history of the rearward cold front prior to 18GMT was uncertain (although it could be traced back to pre-existing low-level baroclinicity evident within the cold air on 4 January in 850mb WBPT fields). At 18GMT the rearward cold front appeared to coincide with a line of developing convective cells which originated marginally east of T. Figs. 7 and 8 show how this front swept rapidly eastwards across southern Britain accompanied by a line of heavy rain and thunderstorms, and introduced colder, drier air.

The double frontal system is consistent with the 850mb WBPT distribution on Fig. 6b, and with the corresponding rainbands on Figs. 8a and 8b. Remote from the vortex centre, the individual fronts may bear little obvious relation to the rainfall distribution (Fig. 8c). However, they continue to mark distinct changes in airmass characteristics. In terms of rainfall the rearward front, which will be shown in section 4 to be shallow, is only conspicuous near the depression centre where potential instability is released by strong upward motion. (In Fig. 8c the fronts are still evident at the surface although wave development within the baroclinic zone aloft has enhanced the rainfall over western France, masking the former correspondence between the rainbands and the fronts.)

4. VERTICAL STRUCTURE AND AIRFLOWS

In this section, physical and dynamical processes accompanying merging of the cold air vortex and frontal cloudband are examined in more detail using the enhanced network of radiosonde soundings between 21GMT 5 January and 03GMT 6 January 1988.

The cross-section in Fig.9 (00GMT 6 January) was taken along the line AB shown in Fig. 5f which intersects the two frontal zones. The 21GMT and 03GMT soundings have been included by displacing them with a velocity of 220deg 35kn (the average movement of C and the wave on F) to keep them in the correct location relative to the moving system. The rearward cold front is defined by a particularly pronounced gradient of WBPT at low levels. Immediately ahead of it is a low level jet (LLJ) which was colocated with a shallow tongue of warm air. A narrow region of marked potential instability therefore preceeded the front, corresponding to the region of thunderstorms over southwest England. The strongest WBPT gradient across the forward front was at middle and upper levels, much of the thermal contrast at low levels

having been destroyed by warm advection ahead of the rearward cold front. The section, with its distinct WBPT boundaries (separated by a shallow region of moist air at low levels) resembles a "split front" (Browning and Monk BM, 1982), with F being the upper cold front and C the surface cold front. However, in the present case the two fronts did not become split by overrunning of dry air aloft as in BM, but were historically two separate systems.

Isentropic analysis (Fig. 10) revealed that the LLJ was part of a secondary conveyor belt flow originating in the shallow moist zone ahead of the rearward cold front (separate from the warm conveyor belt associated with F). As this flow ascended over a cold conveyor belt (CCB) moving westwards ahead of the new warm frontal zone (described in section 3), the potential instability was released giving rise to the deep convection (and associated thunderstorms over south Wales and southeast Ireland). It was this convection (cloud area 2 on Figs. 5a-d) that rapidly bridged the gap between C and F. Continued but less rapid ascent produced the upper cloud canopy which curled around the cold air vortex. Fig. 10 confirms the configuration of the airflows around the cold air vortex depicted in Fig. 1. It also closely resembles a model presented by Browning and Hill (1984) of a summertime mesoscale convective system (MCS) over southwest England. In their case the conveyor belt feeding the MCS consisted of very warm continental air which ascended over a so-called "cool wedge" - a CCB which had crossed over the cool North Sea.

5. COMPARISON WITH A "CLOUD HEAD"

The shape of cloud area C and its position relative to F at the stage of development depicted in Fig. 2c appear similar to the "cloud head" (eg. Fig. 8 of Monk and Bader 1988) that often precedes extreme cyclogenesis. However, C did not exhibit the same layered structure, but was composed of several distinct mesoscale convective elements similar to the comma clouds discussed by Reed and Blier (1986). Cross-sections through both a cloud head and the system in the present case study (Figs. 11a,b.) are used to compare and contrast the structure of the two features. (The low level horizontal gradient of WBPT corresponding to the rearward cold front analyzed by the model (Fig. 11b) is probably not as sharp as the observations in Fig. 9 suggest.)

In both cases there is a marked upper level moisture boundary associated with the forward frontal zone, and a low level jet in warm air immediately ahead of the rearward front. The position of the surface low relative to the main cloud systems is similar in both cases.

A difference between the two sections is the structure of the rearward baroclinic zone. The cloud head on Fig. 11a is a deep baroclinic zone in which the atmosphere has become stable to upright convection. In contrast the cold air vortex of the incipient "instant occlusion" centred near 9 deg. W on Fig. 11b possesses low level baroclinicity within a potentially unstable environment. Therefore it appears that

the difference in texture between the essentially "layered" cloud head and the mainly convective cold air vortex is due to the difference in static stability.

Further cases must be examined in detail to verify whether the observed similarities and differences in structure and appearance between cloud heads and "instant occlusions" can be applied more generally.

6. USE OF IMAGERY TO VALIDATE THE NUMERICAL MODEL GUIDANCE

Guidance from the numerical model forecasts for 00GMT 6 January issued up to 2 days ahead were unclear. Fig. 12 shows a series of model forecasts all verifying at 00GMT 6 January, (which may be compared with the analysis in Fig. 6b). Each run placed differing emphasis on the cold air low and the induced frontal wave. Of those shown, the most successful forecast of the position and depth of the depression near the British Isles was the 36-hour ECMWF prediction (Fig. 12a). The corresponding fine-mesh run (Fig. 12b) correctly forecast cyclogenesis within the cold air, but overdeepened a wave W corresponding to cloud feature A on Fig. 2b.

The least successful forecast was the fine-mesh based on data at 00GMT 5 January (Fig. 12c). Major cyclogenesis was forecast on the forward frontal wave instead of the cold air vortex. Although the position and central pressure of the wave were essentially correct, the forecast pressure gradient near the cold air vortex was very misleading. The corresponding coarse-mesh forecast (Fig. 12d) correctly emphasised the cold air vortex rather than the wave but still failed to deepen it sufficiently.

The fine-mesh initialized at 12GMT 5 January (Fig. 12e) again failed to resolve the intense core of the vortex, but nevertheless forecast the position correctly. The distribution of rainfall was not quite correct in detail over southern England (see Fig 8b).

The fine-mesh also failed to deepen the cold air vortex sufficiently in two of the cases discussed by MYB (10 November 1986 and 9 February 1987) and in the case described by Monk and Bader, 1988.

When producing the forecasts for this exercise of FRONTS87, the run of the fine-mesh at 00GMT 5 January gave strong grounds for suspicion at a very early stage, because considerable organization (and rotation) of the cold air feature was already apparent on Meteosat imagery at 0130GMT (Fig. 13). It also possessed distinct secondary low level baroclinicity and was lying in a strong upper flow (within a sharpening upper trough, Fig. 3a,b) which would carry it towards the polar front. The behaviour of C therefore exhibited the characteristics identified in the forecast guidelines of MYB (chapter 6), and so marked cyclogenesis in the cold air was considered very likely in contrast to the model's forecast. The developing surface low would move northeast in the strong upper flow ahead of the upper trough. Imagery therefore alerted the forecaster almost a day ahead to

a possible alternative solution to that in the model, with a much deeper cold air vortex.

7. CONCLUSIONS

The case study presented in this paper has provided evidence from an enhanced observational network in FRONTS 87 to support the conceptual airflow model of the "instant occlusion" proposed by McGinnigle et al. (1988), and has demonstrated the application of the frontal analysis implied by the model. This case has also demonstrated the viability of other conceptual models, namely the "split-front" (Browning and Monk, 1982), and ascent over a "cool wedge" giving rise to thunderstorms (Browning and Hill, 1984).

Some aspects of the imagery prior to rapid development of the cold air vortex broadly resembled the "cloud-head" but the rearward frontal zone was not nearly as pronounced as in the case presented by Monk and Bader (1988). Nevertheless, mean surface winds of up to 50kn were reported some 9 to 12 hours later. As in the case presented by Monk and Bader, numerical models systematically failed to predict the intense core of particularly strong winds.

Recognition from satellite imagery of the organised cold air feature approaching the frontal zone helped to reconcile conflicting numerical model guidance leading up to the event.

ACKNOWLEDGEMENTS

The author wishes to thank M.J. Bader, J.B. McGinnigle and G.A. Monk for helpful comments on the first manuscript.

REFERENCES

Anderson, R.K., et al., 1969 Application of meteorological satellite data in analysis and forecasting. Tech. Rpt. 212, Air Weather Service, Washington.

Browning, K.A. and Hill, F.F. 1984 Structure and evolution of a mesoscale convective system near the British Isles. Q.J.R. Met. Soc., 110, 897-913.

Browning, K.A. and Hill, F.F. 1985 Mesoscale analysis of a polar trough interacting with a polar front. Quart. J. R. Met. Soc.,111, 445-462.

Browning, K.A. and Monk, G.A. 1982, A simple model for the synoptic analysis of cold fronts. Q.J.R. Met. Soc.,108, 435-452.

Clough, S.A. 1987 The mesoscale frontal dynamics project. Met. Mag., 116, 32-42.

Kurz, M. 1987 Dynamics of stable and unstable baroclinic waves- as described by quasi-geostrophic theory and seen in satellite images. Satellite and radar imagery interpretation. Preprints from a Workshop, Reading, England 20-24 July 1987.

McGinnigle, J.B., Young, M.V. and Bader, M.J. 1988 The development of instant occlusions in the north Atlantic. Met O 15 Internal Report No. 73.

Monk, G.A. and Bader, M.J. 1988 Satellite imagery of the development of the storm of 15-16 October 1987. Weather, 43, 130-135.

Reed, R.J. and Blier, W. 1986 A case study of comma cloud development in the Eastern Pacific. Mon. Wea. Rev.,114, 1681-1695.

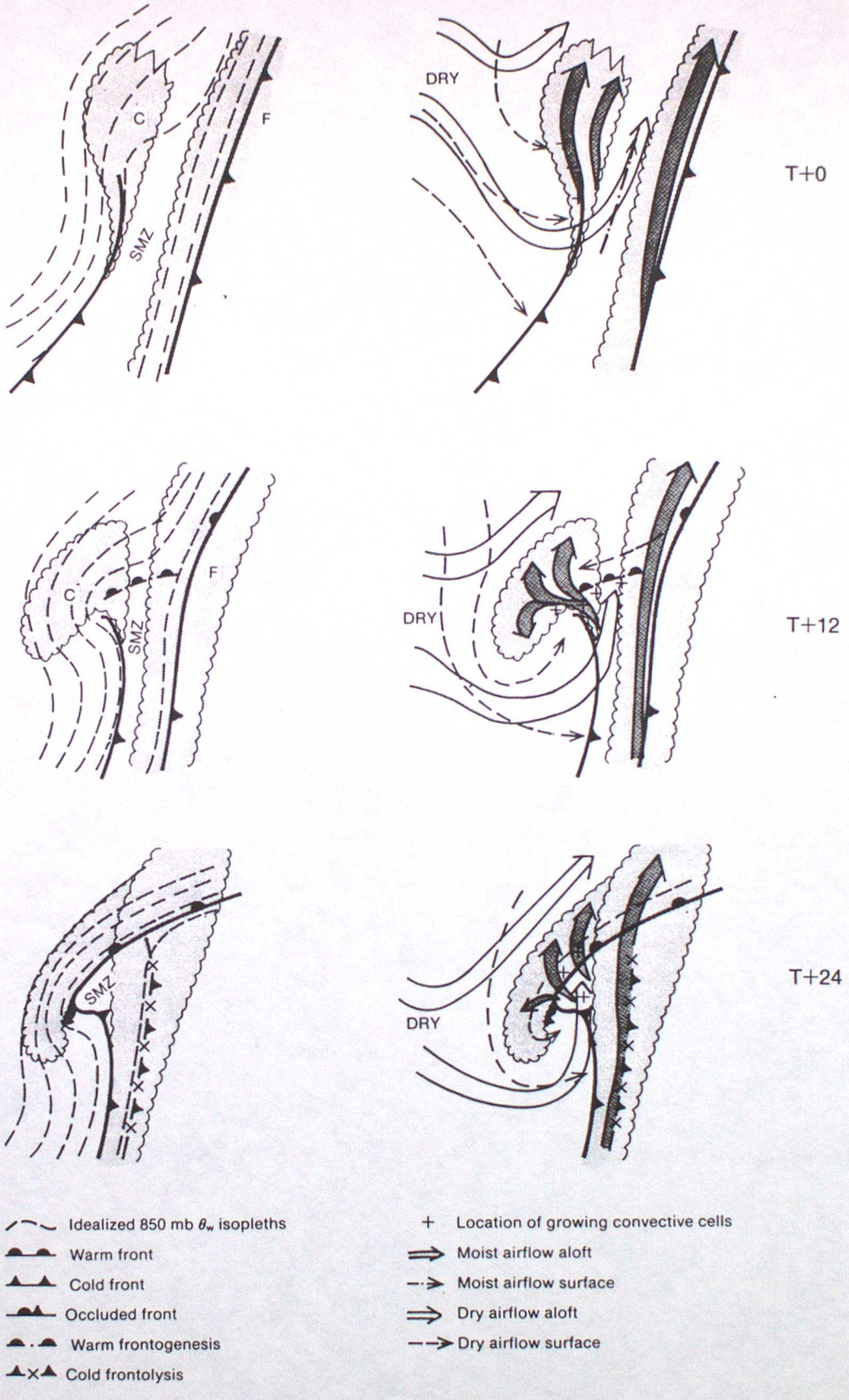

Figure 1

Life cycle model showing interaction between a polar air vortex C and a polar frontal cloud band F at approximately 12 hourly intervals. Broadening and narrowing arrows show ascending and descending air respectively. SMZ denotes shallow moist zone. Stippling represents upper cloud. (Reproduced from McGinnigle et al., 1988)

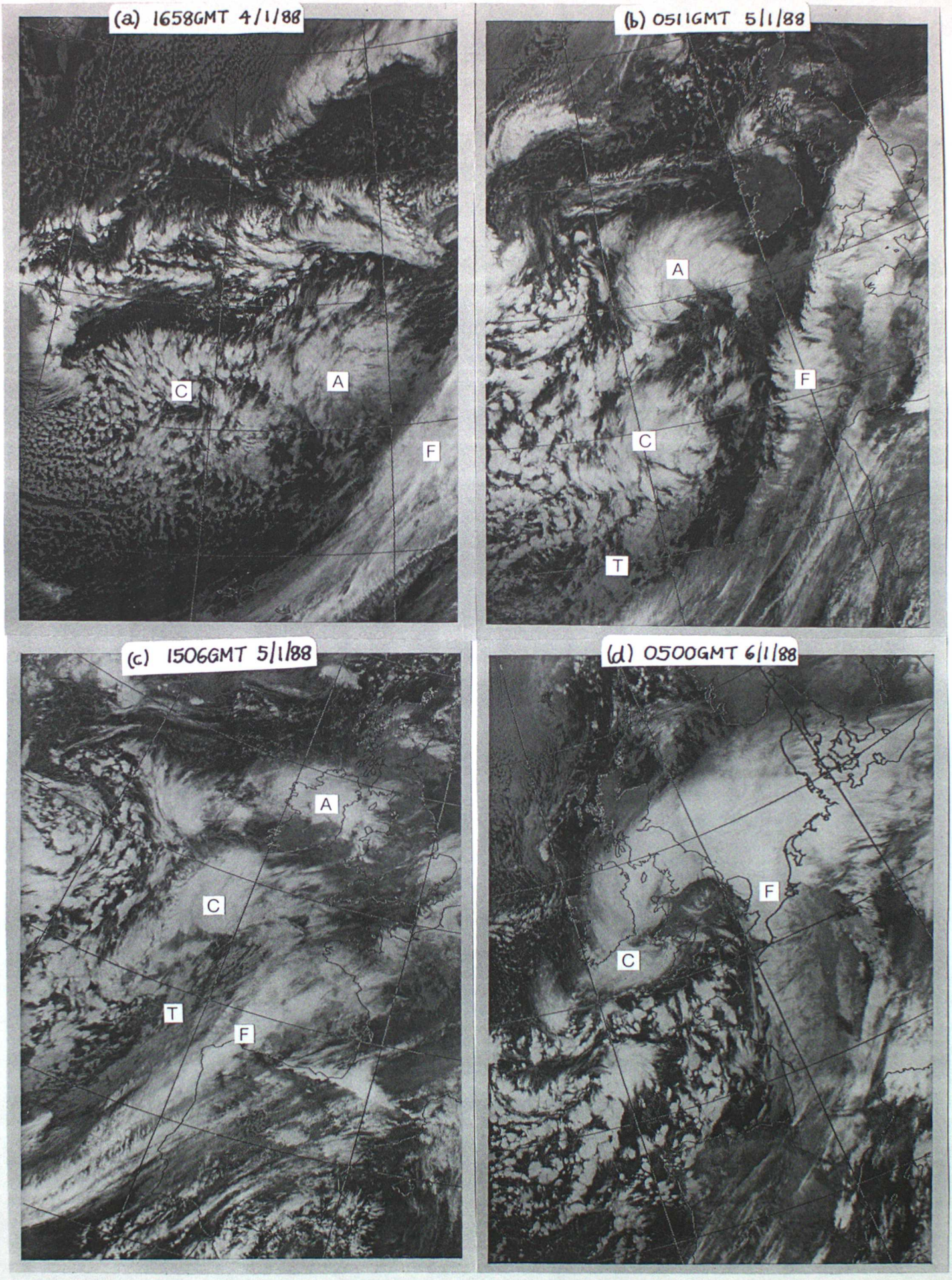

Figure 2

NOAA infra-red satellite images for (a) 1658GMT 4 January 1988, (b) 0511GMT 5 January, (c) 1506GMT 5 January , (d) 0500GMT 6 January. C,F,A and T indicate cloud areas referred to in the text. C and F are cloud features corresponding to those in Fig. 1. (Photographs courtesy of University of Dundee.)

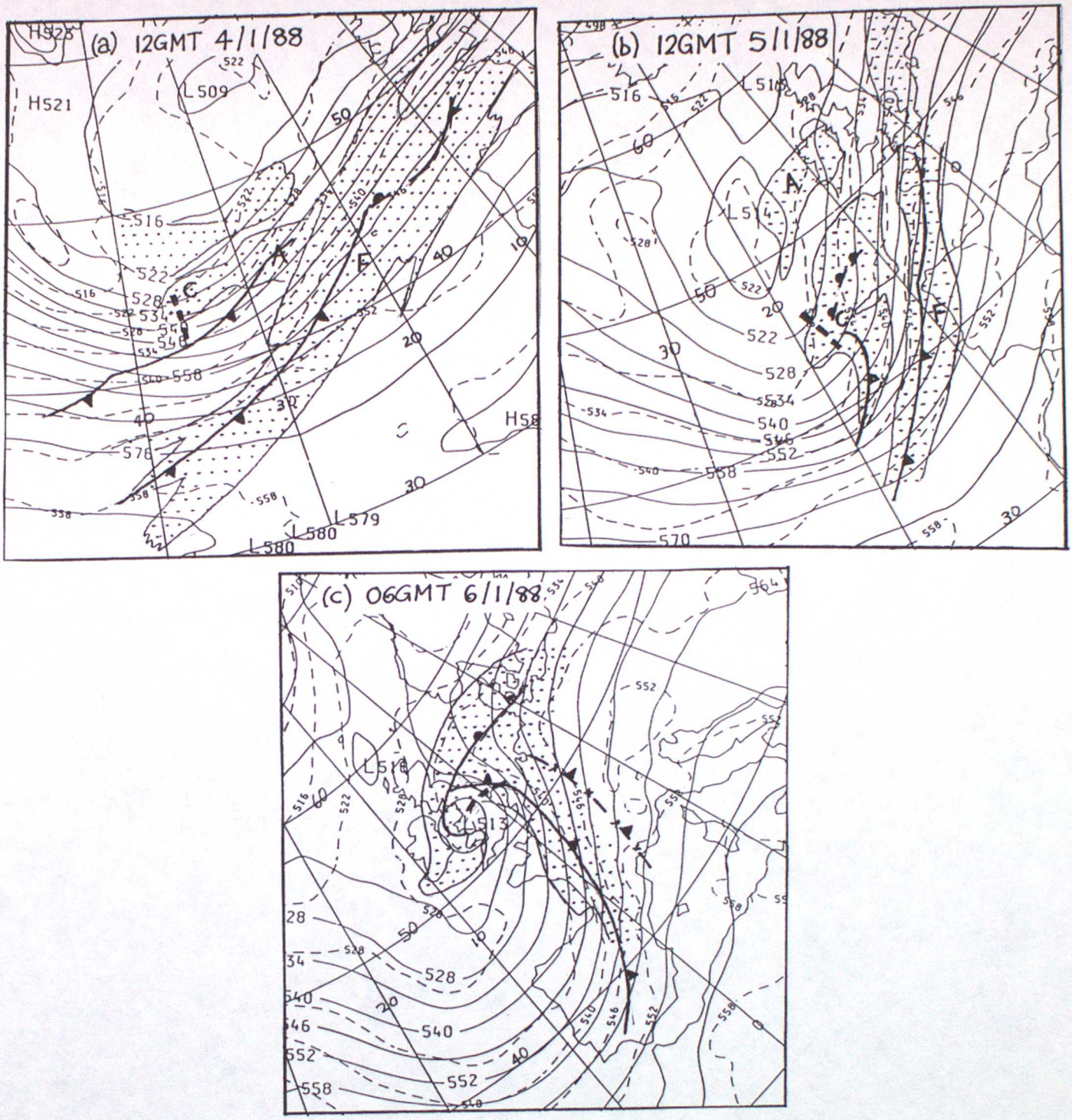

Figure 3

Upper air analyses derived from the fine mesh model for 12GMT 4 January 1988, 12GMT 5 January and 06GMT 6 January. Continuous lines are 500mb heights, and dashed lines are 1000-500mb thicknesses in decametres. Upper cloud areas are stippled. C, F and A are as in Fig. 2. The bold dotted line marks the axis of the short-wave trough associated with C. Surface fronts are also shown.

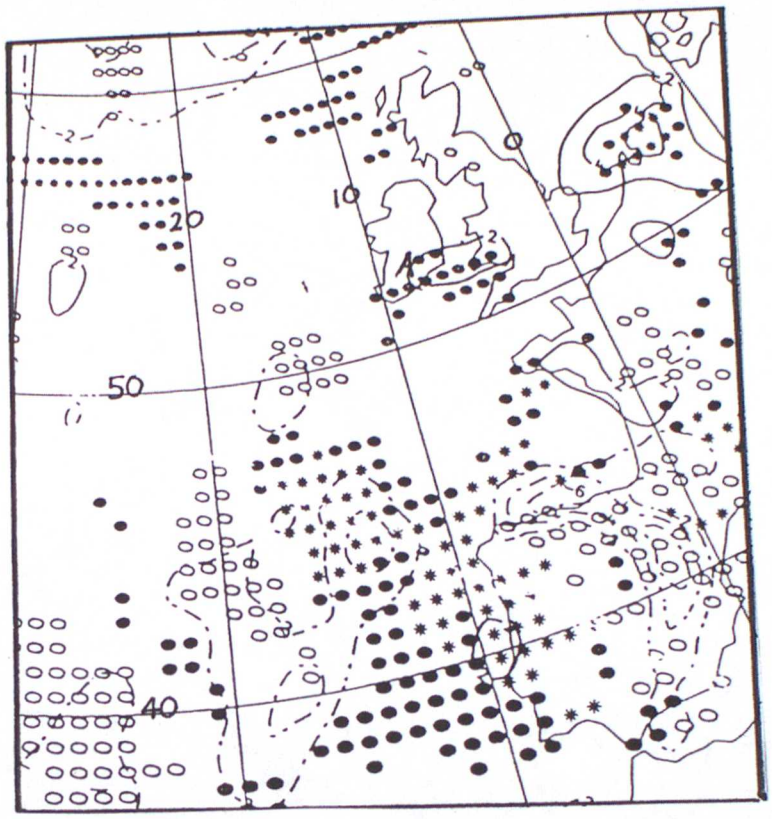

Figure 4

Vertical velocity and thermal advection analysed by the fine-mesh model for 12GMT 5 January 1988, averaged over the 850-500mb layer. Open circles represent descent of more than 6mb/h, closed circles ascent of 6-12mb/h, and asterisks ascent of more than 12mb/h. The isopleths are thermal advection in degrees C per 6 hours, continuous lines being warm advection and dashed lines cold advection. The location of cloud area A is marked.

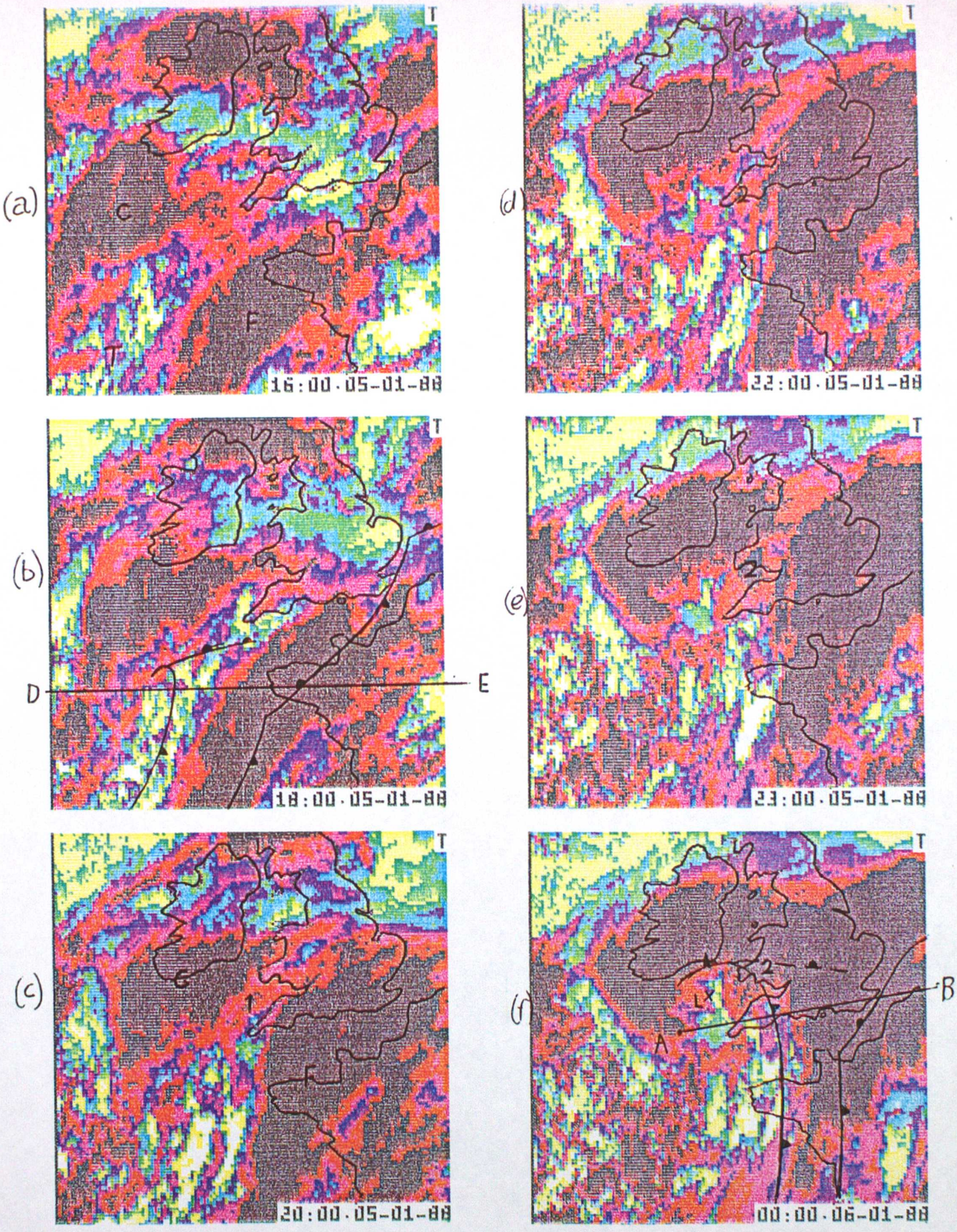

Figure 5

False colour Meteosat infra-red images for 16GMT 5 January to 00GMT 6 January 1988. The colour scheme represents temperature slicing as follows: black, colder than -40deg C, red -30 to-40, mauve, -20 to -30, purple -10 to -20, pale blue 0 to -10, green 0 to 5, yellow 5 to 10, white warmer than 10. C,F,T,1 and 2 are cloud areas referred to in the text. AB and DE are the lines of the cross-sections in Figs. 9 and 11b respectively. T ceases to be identifiable after 16GMT 5 January.

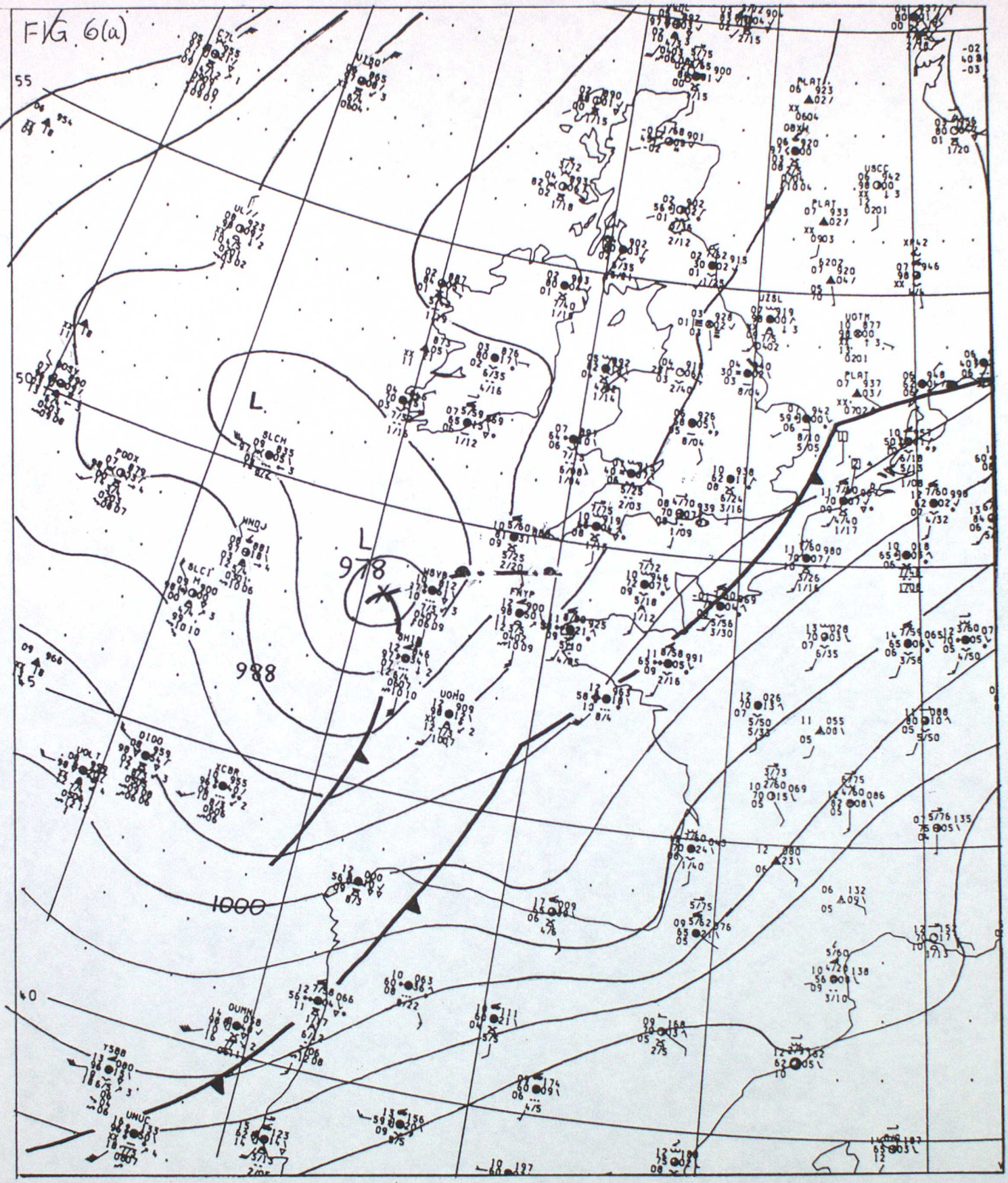

Figure 6

Surface analyses for (a) 18GMT 5 January, (b) 00GMT 6 January. Isopleths of 850mb WBPT are superimposed (dashed) on (b) derived from all available radiosonde data between 21GMT 5 January and 03GMT 6 January. The locations of St. Mawgan S, Aberporth A, Yeovilton Y, and Rennes R are marked in (b).

Figure 6b

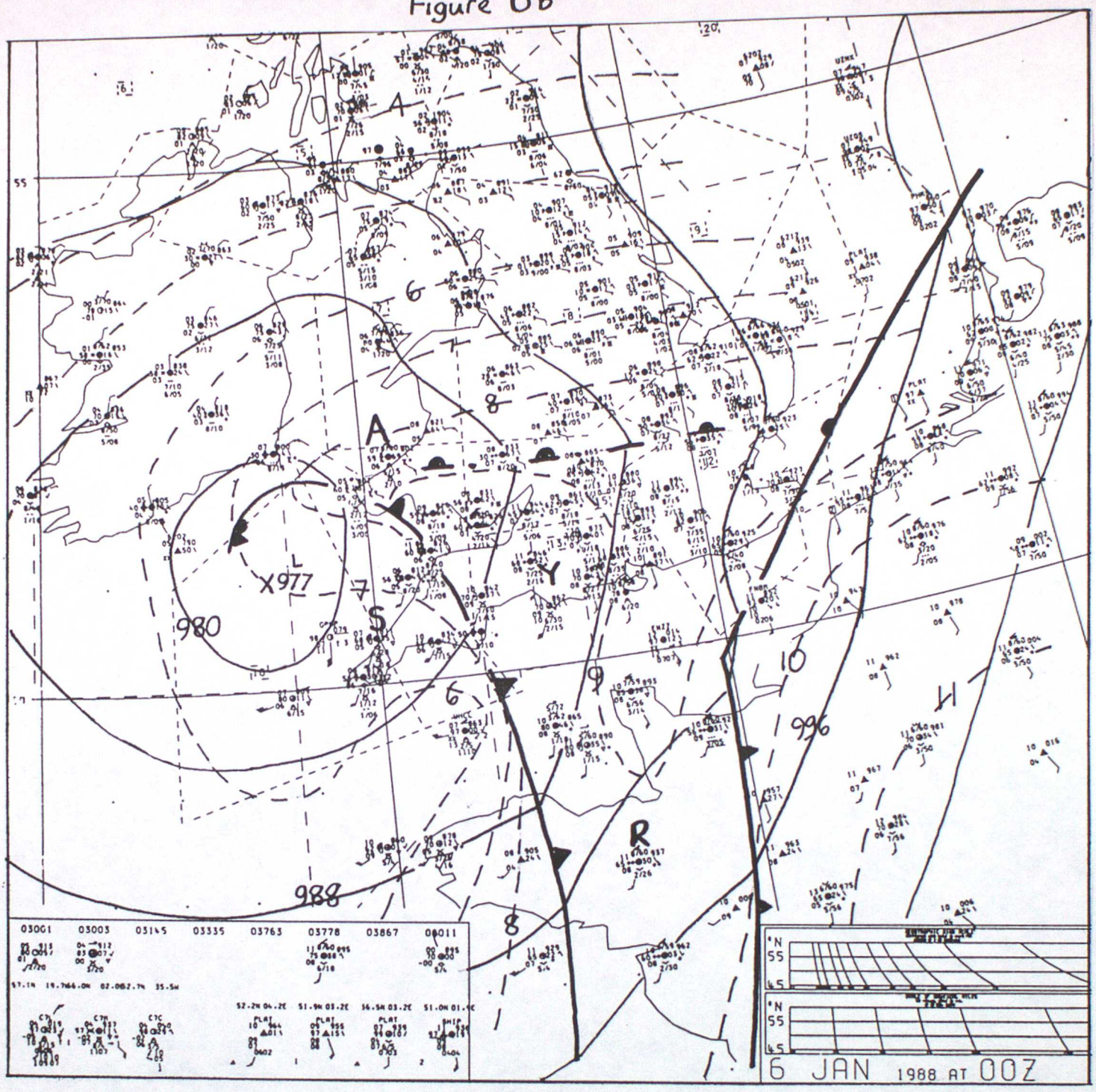

SURFACE OBSERVATIONS 5-6 JANUARY 1988

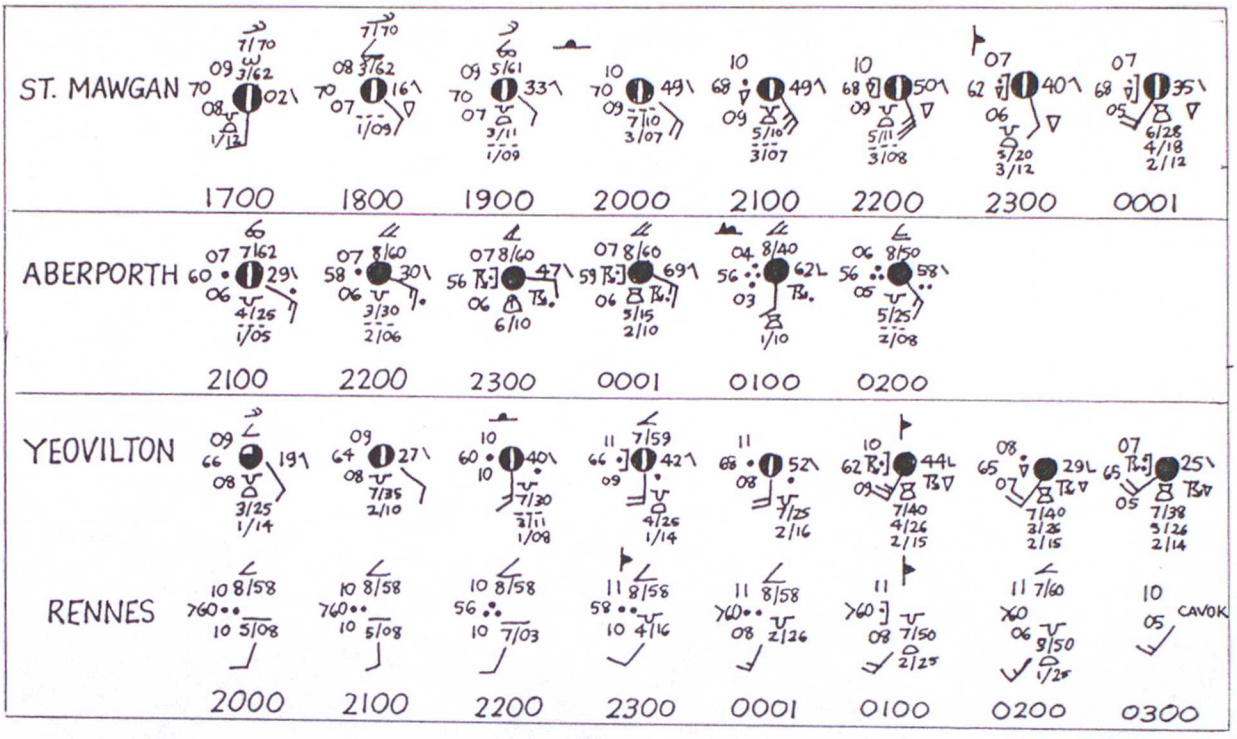

Figure 7

Sequence of hourly surface observations from St. Mawgan, Aberporth, Yeovilton, and Rennes, the locations of which are shown in Fig. 6b as S, A, Y and R respectively. Observations from Rennes are based on METAR reports. Times (GMT) are shown below the observations. Frontal passage is indicated by the appropriate frontal symbols.

Fig 8a

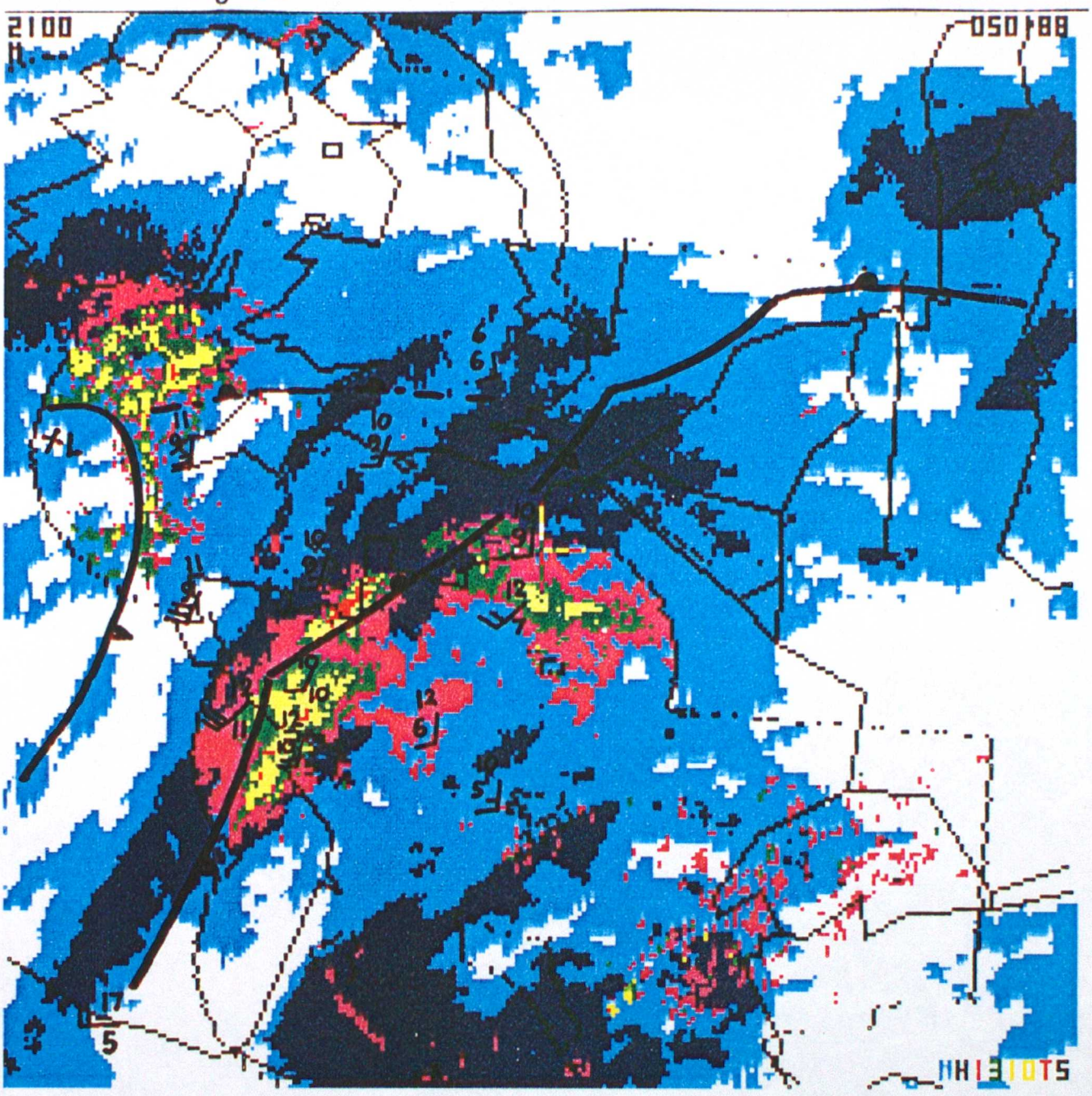

Figure 8

Combined Meteosat and radar imagery from the European COST73 network for (a) 21GMT 5 January, (b) 00GMT 6 January, (c) 03GMT 6 January. Temperature slicing is as follows: dark blue colder than -45deg C, pale blue -20 to -45, white warmer than -20. Rainfall rates are as follows: pink less than 1mm/hr, green 1-3mm/hr, yellow, 3-10mm/hr, red 10-32mm/hr. Surface fronts and synoptic observations are shown conventionally. On (b) the French radar data are missing.

Fig 8b

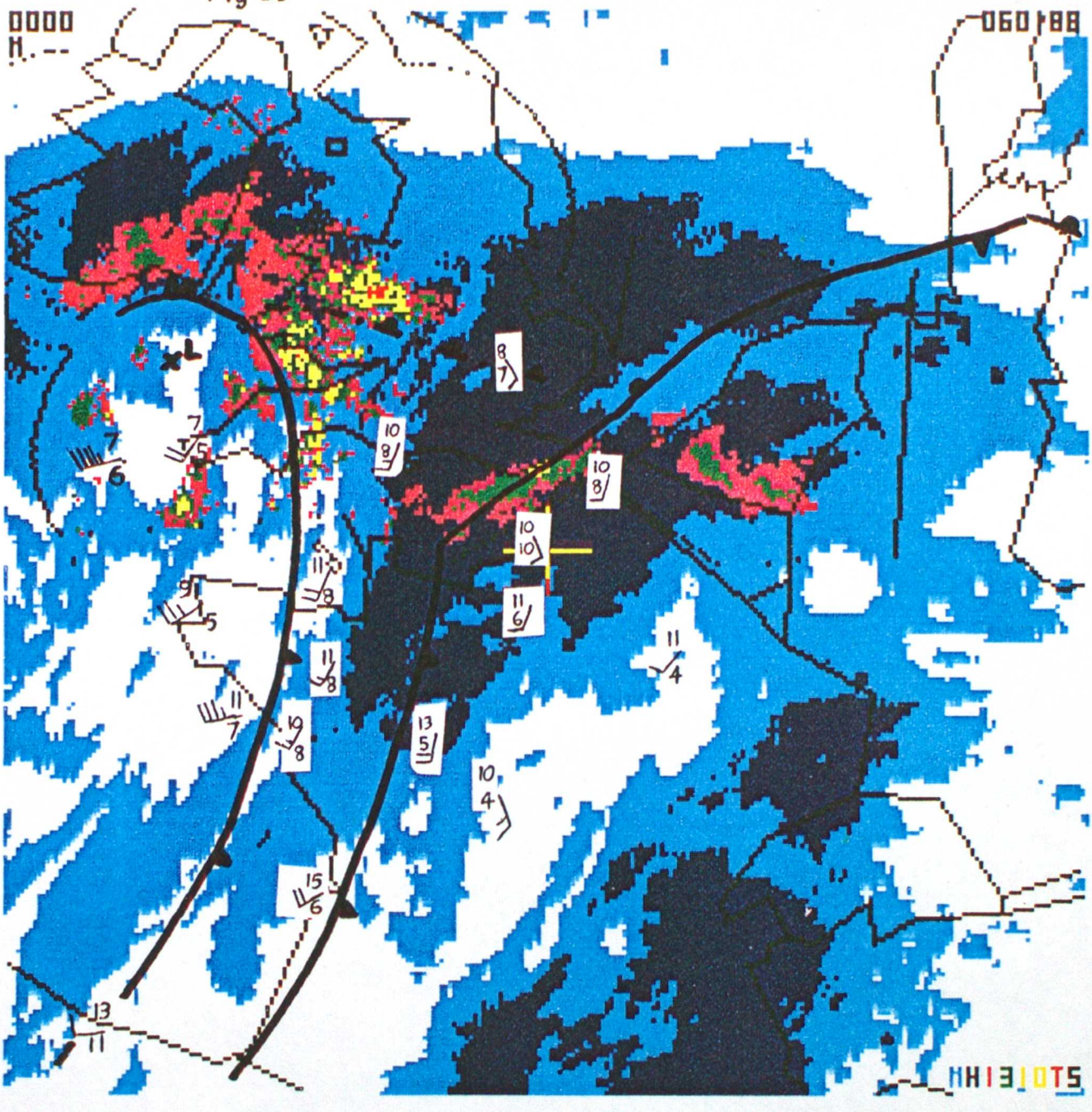
0000
H.--
0601 88
8
7
10
8
10
8
10
10
11
6
11
4
11
8
11
8
11
7
9
8
13
5
10
4
15
6
13
11
7
6
7
5
9
5
STOIEIHH

Fig 8c

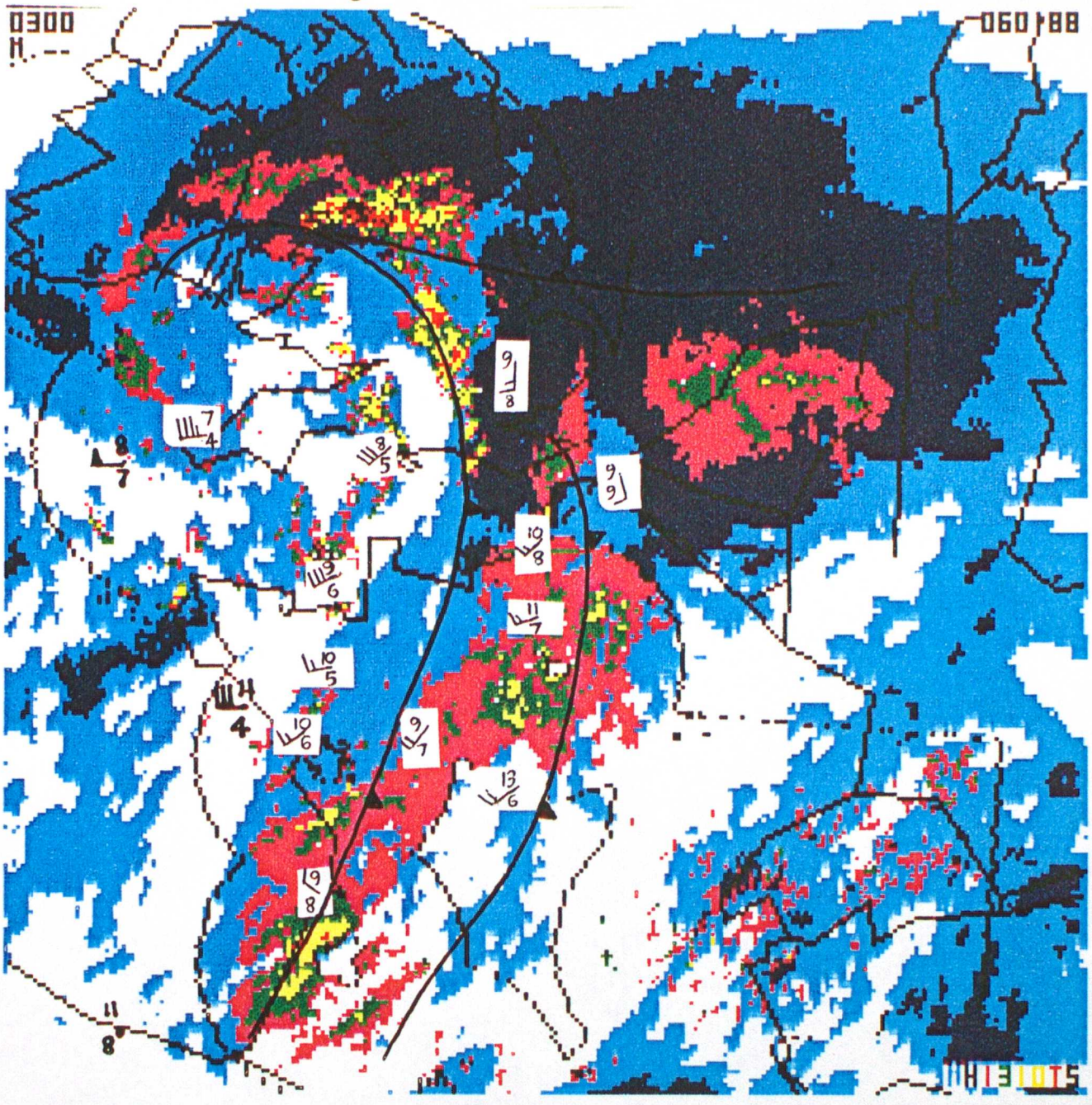

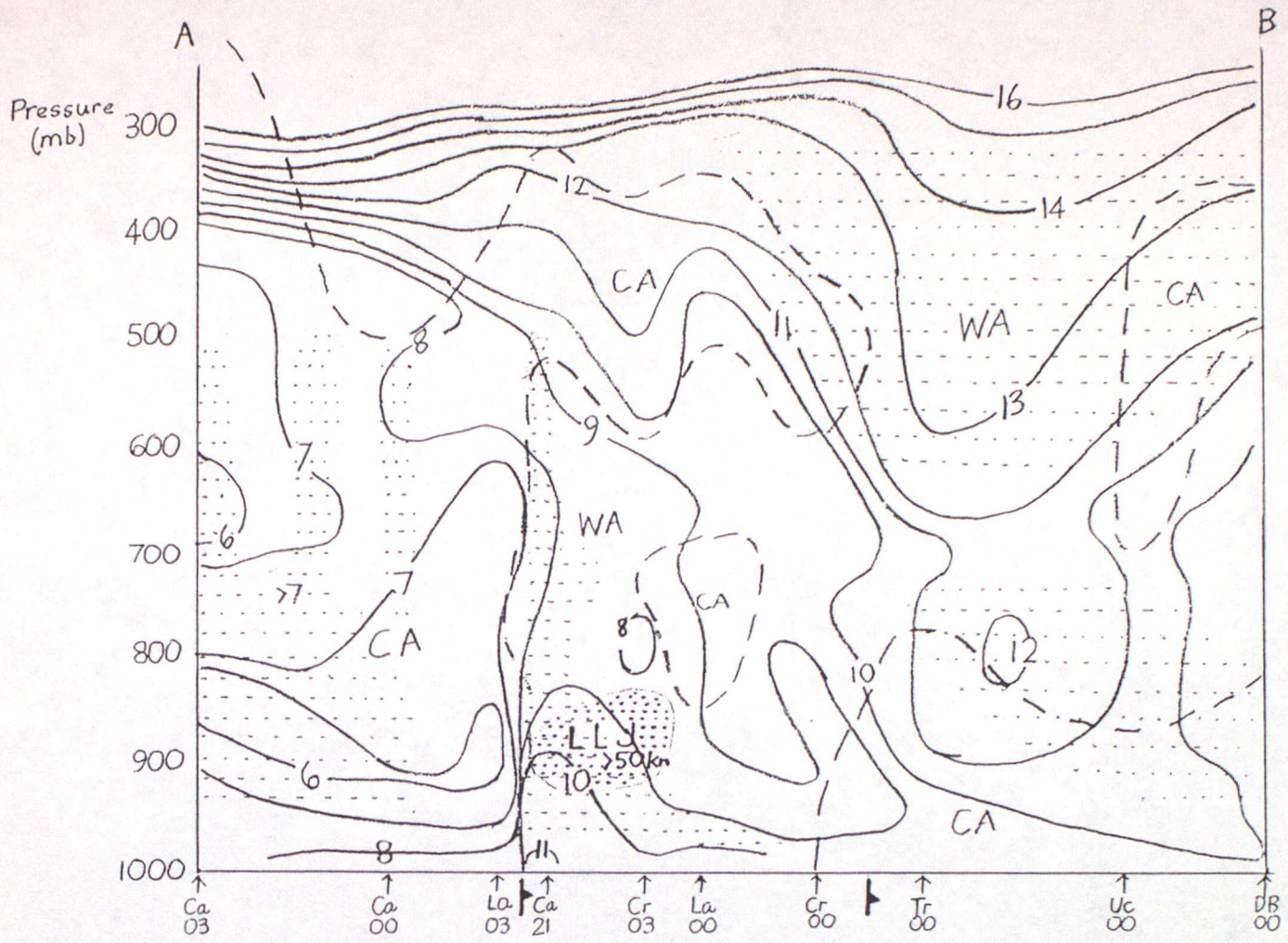

KEY

Cloud and/or >90% humidity

Winds >50kn within low level jet

$\sim \theta_w$

– – – Zero thermal advection

CA Cold advection
WA Warm advection
LLJ Low level jet

Figure 9

Cross-section along the line AB in Fig. 5f valid at 00GMT 6 January derived from radio-sonde observations. Continuous lines are WBPT (C), dashed lines represent zero thermal advection. Areas of warm and cold advection are identified by WA and CA respectively. Light stippling represents areas of cloud and/or greater than 90% relative humidity. Heavy stippling depicts winds over 50kn within the low-level jet, LLJ. The locations of radiosonde soundings projected on to the line of the section are shown on the horizontal axis along with the time (GMT) of the observation. The abbreviations are as follows: Camborne Ca, Crawley Cr, Larkhill La, Trappes Tr, Uccle UC, and De Bilt DB.

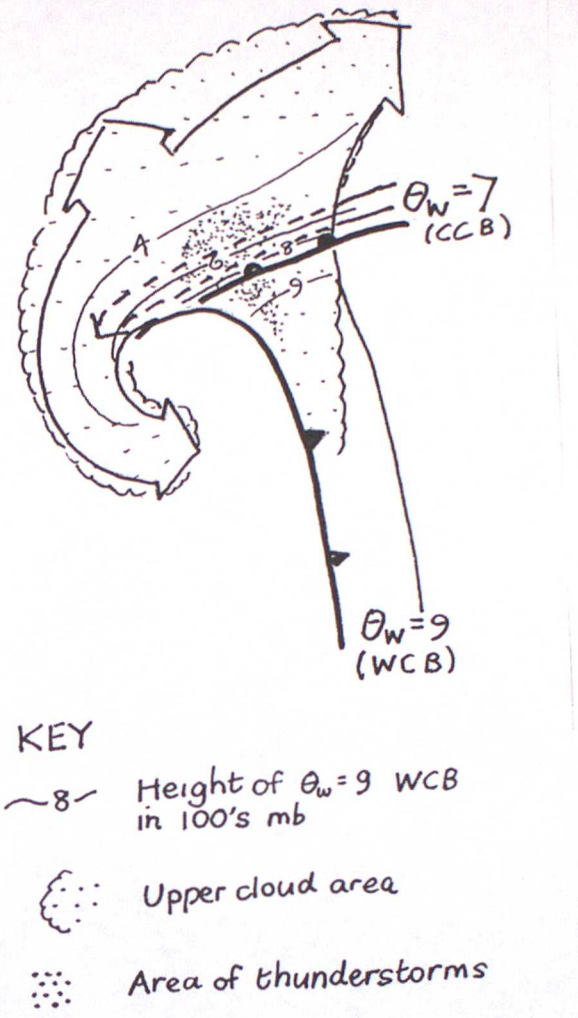

Figure 10

Airflows relative to the movement of of the cold air vortex at 00GMT 6 January, derived by isentropic analysis. The conveyor belt (solid arrow), characterized by the flow on the 9 deg. C WBPT surface, originates ahead of the cold front and rises abruptly over the new warm frontal surface. The resulting release of potential instability causes the area of thunderstorms (stippled). The cold conveyor belt (dotted arrow) is associated with the 7 deg. WBPT surface. The warm conveyor belt corresponding to F is further east and is not shown. Upper cloud areas are shown by light stippling within a cusped line.

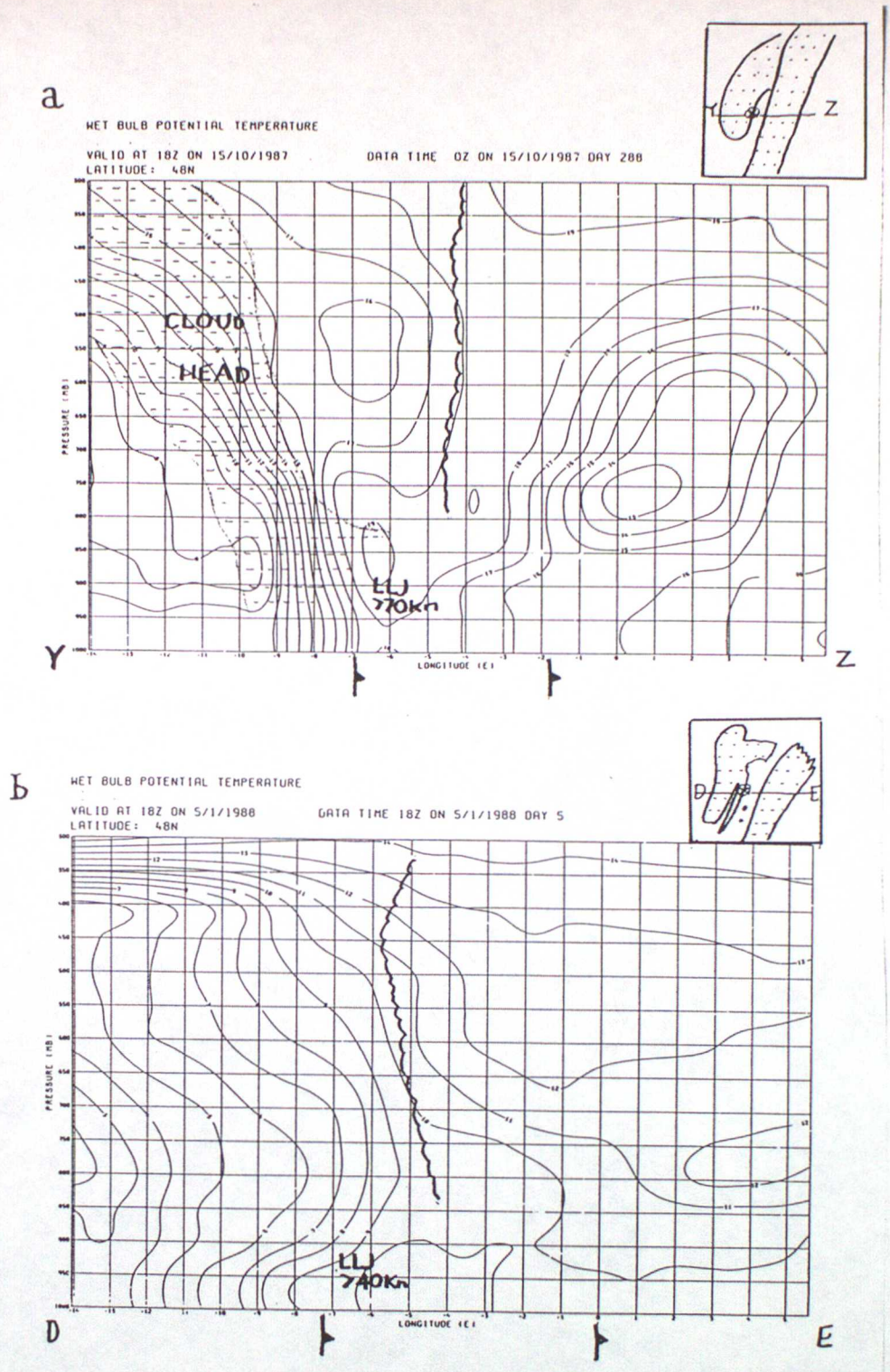

Figure 11

Fine mesh model cross-section from longitude 14W to 5E (a) along the line YZ across a cloud head at 18GMT 15 October 1987, and (b) along the line DE in Fig. 5b. Continuous lines are WBPT (deg. C). The insets are schematic diagrams of the main cloud features (stippled) showing the line of the cross-section and the location of the surface low (circled cross). The cusped line is the rear edge of the upper level moisture boundary (defined by 90% RH) associated with the forward front. LLJ denotes location and northward component of speed of the low-level jet. Moist air with RH greater than 90% comprising the cloud head is stippled in (a). In neither case is the forward front evident in the WBPT field since at low levels the warmer air to the east is drier than the colder air to the west. However, it could be placed using surface wind observations and temperature sections. The overall appearance of (b) strongly resembles sections through similar systems eg. Fig. 16 of MYB.

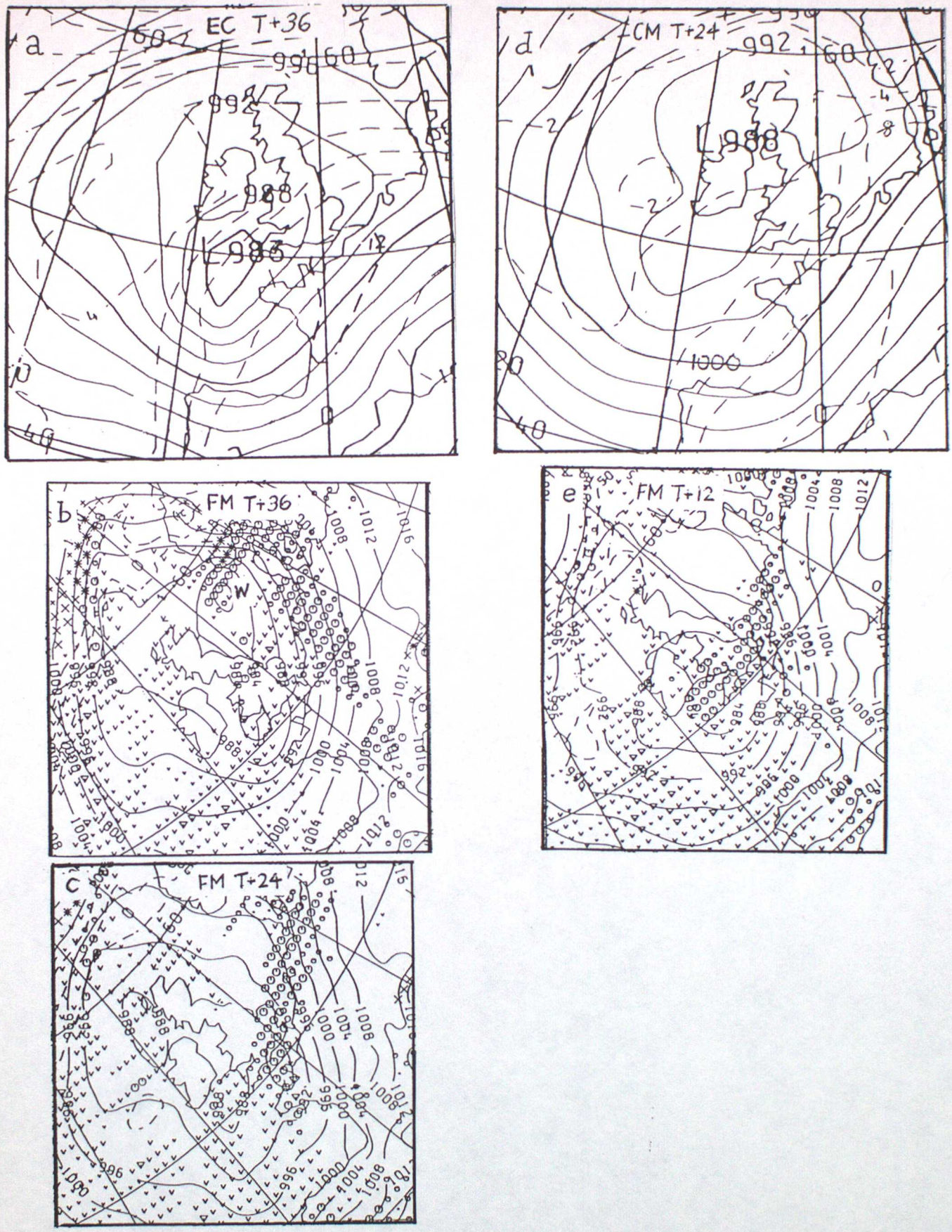

Figure 12

Forecasts of mean sea level pressure (continuous lines) verifying at 00GMT 6 January 1988. (a) ECMWF 36-hour forecast; (b) fine mesh 36-hour forecast; (c) fine mesh 24-hour forecast; (d) coarse mesh 24-hour forecast; (e) fine mesh 12-hour forecast. In (a) dashed lines are 850mb WBPT. In (b),(c) and (e) dots, small and large circles represent rainfall rates of less than 0.1mm/hr, 0.1-0.5 mm/hr, and 0.5-4.0mm/hr respectively. Increasing sized V symbols represent the same threshold of local convective rainfall rates, whilst triangles are rates exceeding 4mm/hr. In (b) W is referred to in the text.

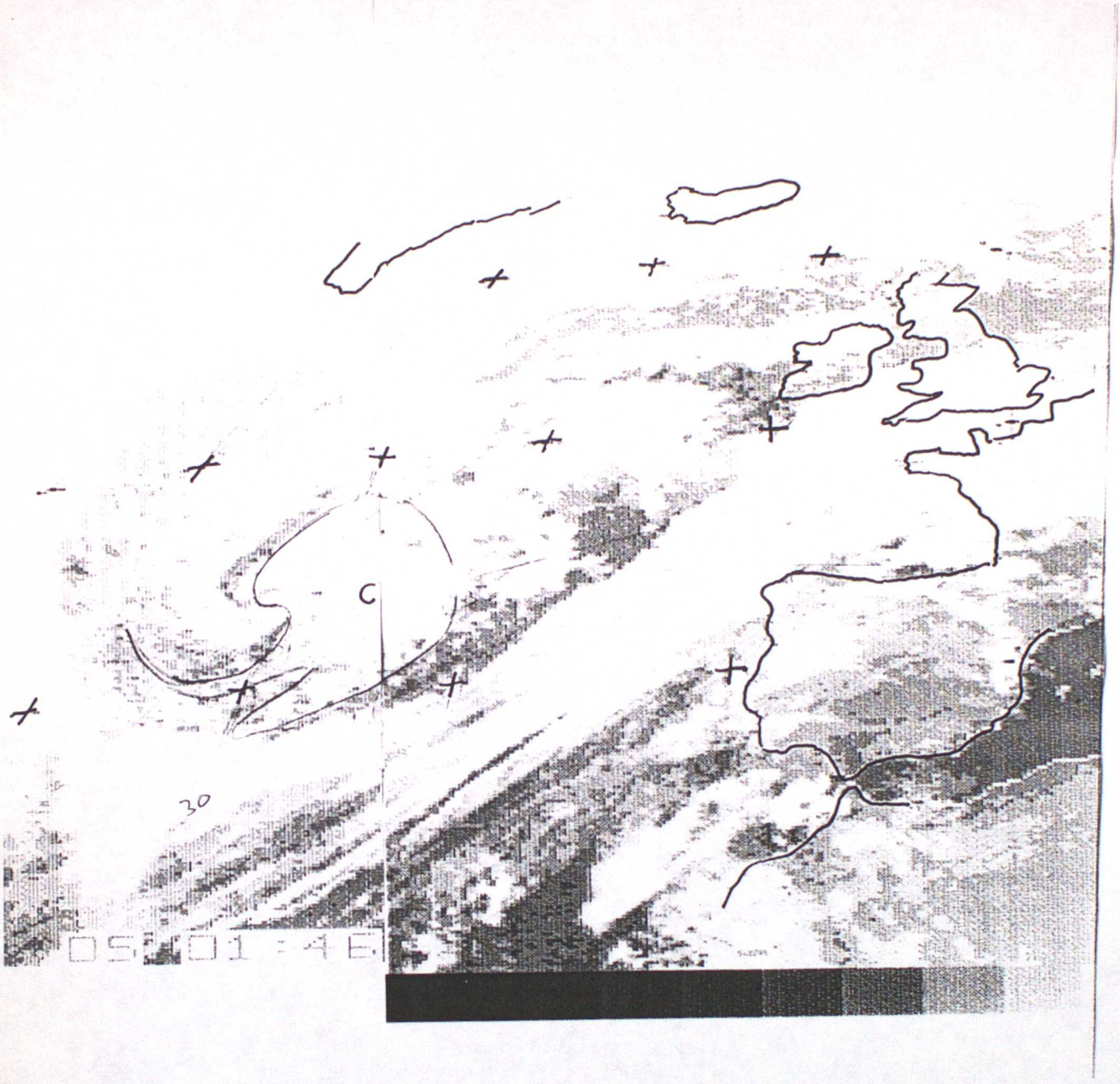

Figure 13

Meteosat infra-red image for 0130GMT 5 January 1988. Cloud area C is labelled.